ELSEVIER

Biochimica et Biophysica Acta 1463 (2000) 395–406

BIOCHIMICA ET BIOPHYSICA ACTA
BBA

www.elsevier.com/locate/bba

Liquid crystalline/gel state phase separation in docosahexaenoic acid-containing bilayers and monolayers

Alfred C. Dumaual, Laura J. Jenski, William Stillwell *

Department of Biology, Indiana University-Purdue University at Indianapolis, 723 W. Michigan Street, Indianapolis, IN 46202-5132, USA

Received 8 July 1999; received in revised form 11 November 1999; accepted 16 November 1999

Abstract

The phase behavior of lipid mixtures containing 1-stearoyl-2-docosahexaenoyl-*sn*-glycero-3-phosphocholine (18:0, 22:6 PC) with 1,2-dipalmitoyl-*sn*-glycero-3-phosphocholine (DPPC) was studied with bilayers using differential scanning calorimetry (DSC), and with monolayers monitoring pressure/area isotherms and surface elasticity, and lipid domain formation followed by epifluorescence microscopy. From DSC studies it is concluded that DPPC/18:0, 22:6 PC phase separates into DPPC-rich and 18:0, 22:6 PC-rich phases. In monolayers, phase separation is indicated by changes in pressure–area isotherms implying phase separation where 18:0, 22:6 PC is 'squeezed out' of the remaining DPPC monolayer. Phase separation into lipid domains in the mixed PC monolayer is quantified by epifluorescence microscopy using the fluorescently labeled phospholipid membrane probe, 1,2-dioleoyl-*sn*-glycero-3-phosphoethanolamine-*N*-(lissamine rhodamine B sulfonyl). These results further describe the ability of docosahexaenoic acid to participate in lipid phase separations in membranes.

Keywords: Lipid phase separation; Lipid microdomain; Lipid monolayer; Docosahexaenoic acid; Squeeze out

1. Introduction

It has been proposed that lipids and proteins in biological membranes are distributed heterogeneously throughout the bilayer in discrete patches known as domains [1,2]. Membrane domains can fall under two general categories, protein-driven macrodomains and lipid-driven microdomains. Protein macrodomains are membrane structures based on protein–protein interactions where lipids are associated secondarily [3]. Examples of protein macrodomains include focal contacts, nerve synapses, and basal and apical poles of endothelial cells [2]. These membrane structures can be visualized, and are long-lived and generally well characterized.

Much less understood are the lipid microdomains which probably constitute the majority of most membranes and would be formed by lipid–lipid and lipid–protein interactions [4–6]. The question remains, if lipid domains do exist, do they play a significant role in normal cellular function? Recently membrane fractions that are insoluble in cold Triton X-100 (called DRM, detergent resistant membranes) have been isolated and characterized [7–9]. DRMs are cur-

Abbreviations: DPPC, 1,2-dipalmitoyl-*sn*-glycero-3-phosphocholine; 18:0, 22:6 PC, 1-stearoyl-2-docosahexaenoyl-*sn*-glycero-3-phosphocholine; MLV, multilamellar vesicles; *N*-Rh-DOPE; 1,2-dioleoyl-*sn*-glycero-3-phosphoethanolamine-*N*-(lissamine rhodamine B sulfonyl)

* Corresponding author. Fax: +1-317-274-2846;
E-mail: wstillwe@iupui.edu

0005-2736/00/$ – see front matter
PII: S0005-2736(99)00235-7

rently the best example of lipid microdomains isolated from biological membranes. They are apparently microdomain remnants extracted from the parent membrane and are composed largely of cholesterol and sphingolipids in the liquid ordered (l_o) state [7–9]. Unfortunately almost nothing is known about the number, size, composition and half-life of the microdomains found in the parent membranes from which DRMs are obtained [5].

Lipid microdomains have also been investigated in model membranes. The best studied of the model systems are those with co-existing gel/liquid-crystalline state phospholipids [10–13]. While easy to demonstrate phase separation, these systems have the disadvantage of limited biological relevance. Significant levels of gel state are found in only a few biological membranes, including sperm plasma membrane [14], and in *Achoelplasma laidlawii* [15] and *Escherichia coli* [16] that had been supplemented with saturated fatty acids. Furthermore, gel state lipids are selectively exfoliated from some membranes under physiological conditions [17,18]. Interestingly, the l_o state of cholesterol and sphingolipid-rich DRMs does resemble the gel state of DPPC bilayers. Like DPPC and other gel state lipids, the acyl chains of SM occurring naturally are mostly saturated [6], and both lipids have a high affinity for cholesterol compared to other phospholipid species [6,12,19,20]. The high phase transition temperature of SM ($\sim$40°C) is similar to DPPC (42.4°C) [6]. Gel state DPPC like SM was also found to be Triton-insoluble [21,22]. Similarities in physical properties have allowed use of DPPC as a model to study sphingomyelin in bilayers [23]. Studies of liquid crystalline/gel state bilayers, similar to those that are presented here, may then be applicable to phase separations occurring in biological membranes containing cholesterol- and sphingolipid-rich DRMs.

The basis of lipid microdomain formation is likely related to the strength of lipid–lipid or lipid–protein interactions that may occur in the membrane. Lipid interactions are based on head group and/or acyl chain affinities [24]. Previous studies have shown that acyl chain composition (chain length and number of double bonds) could be a driving force for lipid interactions [25,26]. Of particular interest here is the long chain, polyunsaturated ω-3 fatty acid, docosahexaenoic acid (DHA, $22{:}6^{\Delta 4,7,10,13,16,19}$) and how it may affect membrane properties when incorporated into phospholipids. DHA is the longest and most unsaturated fatty acid commonly found in biological membranes [27]. It is likely that DHA-containing phospholipids alter membrane structure, thus affecting membrane function [28,29]. Here we employ the techniques of differential scanning calorimetry (DSC) on lipid bilayers (liposomes) and pressure/area isotherms and fluorescence digital imaging microscopy on lipid monolayers to extend prior studies suggesting that DHA may be involved in lipid microdomain formation in biological membranes [19,28].

2. Materials and methods

The phospholipids DPPC (1,2-dipalmitoyl-*sn*-glycero-3-phosphocholine); 18:0, 22:6 PC (1-stearoyl-2-docosahexaenoyl-*sn*-glycero-3-phosphocholine); and *N*-Rh-DOPE (1,2-dioleoyl-*sn*-glycero-3-phosphoethanolamine-*N*-(lissamine rhodamine B sulfonyl) were purchased from Avanti Polar Lipids (Alabaster, AL). The membranes described in these experiments were composed of two phospholipids, DPPC (gel state)/18:0, 22:6 PC (liquid crystalline state) in the following mol ratios: a, DPPC; b, DPPC 90 mol%/18:0, 22:6 PC 10 mol%; c, DPPC 80 mol%/18:0, 22:6 PC 20 mol%; d, DPPC 70 mol%/18:0, 22:6 PC 30 mol%; e, DPPC 60 mol%/18:0, 22:6 PC 40 mol%; f, DPPC 50 mol%/18:0, 22:6 PC 50 mol%; g, DPPC 40 mol%/18:0, 22:6 PC 60 mol%; h, DPPC 30 mol%/18:0, 22:6 PC 70 mol%; i, DPPC 20 mol%/18:0, 22:6 PC 80 mol%; j, DPPC 10 mol%/18:0, 22:6 PC 90 mol%; and k, 18:0, 22:6 PC. The letter designation for each lipid mol ratio is the same for every experiment whether data for that lipid mixture is shown or not.

2.1. Differential scanning calorimetry

Organic solvents were removed from the appropriate membrane phospholipids by evaporation in nitrogen followed by 12 h under vacuum. Multilamellar vesicles (MLV) were made by hydrating overnight the appropriate phospholipids at 10 mg/ml in 10 mM sodium phosphate, pH 7.0 and then oxygen was removed by purging the solution with nitrogen.

All buffers were made from deionized water that was glass distilled and further purified with an Ultrapure Milli-Q water system. MLV were passed through three freeze (liquid nitrogen)/thaw (50°C) cycles. Aliquots of 500 μl of the MLV suspensions were added to each of the three DSC chambers with the fourth chamber containing 500 μl of the buffer. Heating and cooling scans were made at 5°C/h in a Hart Scientific differential scanning calorimeter (Provo, UT). Although only the cooling scans are presented, we could detect only small, inconsequential differences in the T_c, ΔH and cooperativity between the two scans. The cooling curves are presented as *positive* displacements to facilitate comparison between the various lipid mixtures.

2.2. Langmuir trough

Pressure/area (Π–A) isotherms were obtained for phospholipid monolayers at 25°C on a KSV minitrough (KSV Instruments, Helsinki, Finland) using a Wilhelmy plate. Phospholipid monolayers (1.0 mg lipid/ml) were spread with hexane/2-propanol (3:2) as the carrying solvent. The carrying solvent was allowed to evaporate for 15 min before compressions began. The aqueous subphase was 10 mM sodium phosphate, pH 7.0 and compression rates were 1 mN/m.

Surface elasticity moduli (C_s^{-1}) were calculated from the Π–A data obtained from the monolayer compressions using the following equation [30,31]:

$$C_s^{-1} = -(d\Pi/d\ln A) \quad (1)$$

where A is the area per molecule at the indicated surface pressure (Π).

2.3. Epifluorescence microscopy

Phospholipid monolayers on the Langmuir trough were visualized using a Nikon Diaphot inverted phase microscope (Garden City, NY) and imaged using a Dage-MTI CCD-72 camera (Michigan City, IN) interfaced to a Scion LG-3 frame grabber (Frederick, MD) installed on a Macintosh IIx computer. All fluorescent images used the probe, *N*-Rh-DOPE at a probe:lipid ratio of 1:100. Images were quantified using NIH Image software. Fifteen random images were taken at 30-s intervals at a given pressure for each lipid mixture. Images were taken starting at 5-mN/m pressure up to 40 mN/m at 5-mN/m intervals. The % dark was calculated for each image and the total dark area was compared to the total area of the image.

3. Results

Differential scanning calorimetry (DSC) was used

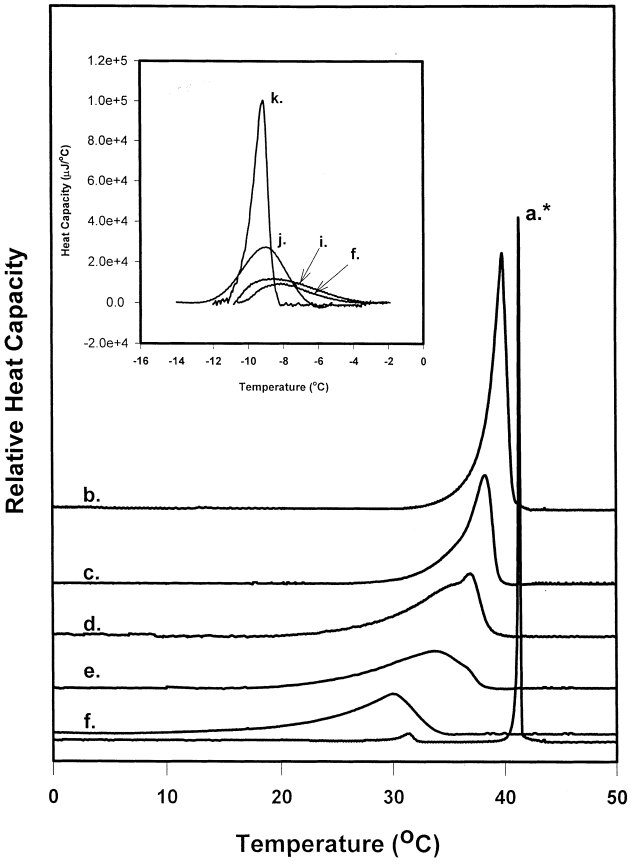

Fig. 1. Differential scanning calorimetry scans of MLV made from mixtures of DPPC/18:0, 22:6 PC. Main figure (higher melting component): curve a, 100 mol% DPPC; curve b, 90 mol% DPPC/10 mol% 18:0, 22:6 PC; curve c, 80 mol% DPPC/20 mol% 18:0, 22:6 PC; curve d, 70 mol% DPPC/30 mol% 18:0, 22:6 PC; curve e, 60 mol% DPPC/40 mol% 18:0, 22:6 PC; and curve f, 50 mol% DPPC/50 mol% 18:0, 22:6 PC. Insert: curve f, 50 mol% DPPC/50 mol% 18:0, 22:6 PC; curve i, 20 mol% DPPC/80 mol% 18:0, 22:6 PC; curve j, 10 mol% DPPC/90 mol% 18:0, 22:6 PC; and curve k, 100 mol% 18:0, 22:6 PC. Curves for mixtures g and h are similar in shape and size to 50 mol% DPPC/50 mol% 18:0, 22:6 PC (curve f) and are not shown.

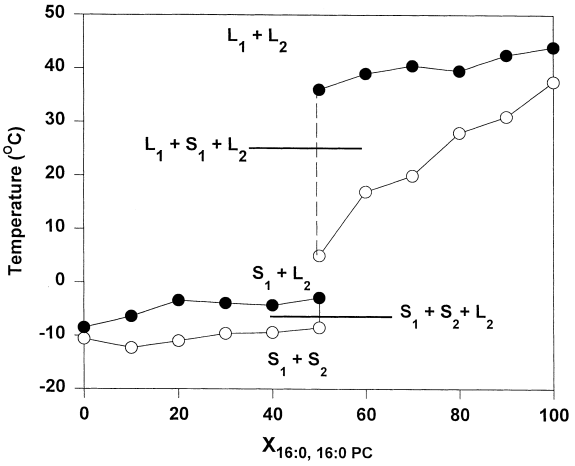

Fig. 2. Partial phase diagram of DPPC/18:0, 22:6 PC mixed bilayers as determined from the DSC curves presented in Fig. 1. Lipid states are described as: L, liquid crystalline; and S, gel. 1 is DPPC and 2 is 18:0, 22:6 PC [32].

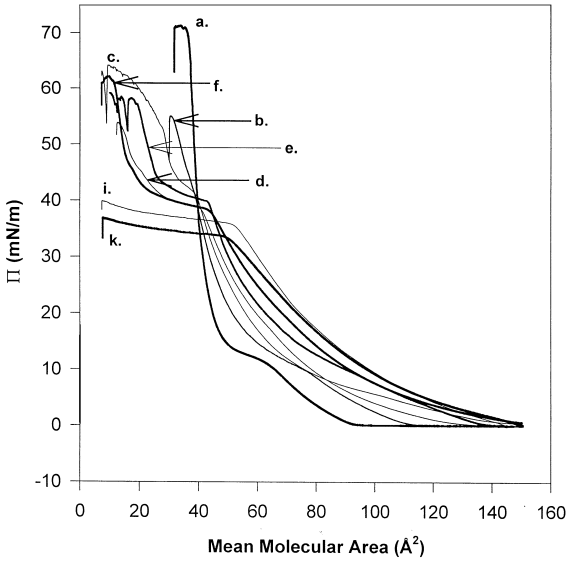

Fig. 3. Pressure–area (Π–A) isotherms of monolayers composed of various mixtures of DPPC/18:0, 22:6 PC. Curve a, 100 mol% DPPC; curve b, 90 mol% DPPC/10 mol% 18:0, 22:6 PC; curve c, 80 mol% DPPC/20 mol% 18:0, 22:6 PC; curve d, 70 mol% DPPC/30 mol% 18:0, 22:6 PC; curve e, 60 mol% DPPC/40 mol% 18:0, 22:6 PC; curve f, 50 mol% DPPC/50 mol% 18:0, 22:6 PC; curve i, 20 mol% DPPC/80 mol% 18:0, 22:6 PC; curve k, 100 mol% 18:0, 22:6 PC.

to detect phase separation with bilayers composed of DPPC ($T_c = 42.4$°C) and 18:0, 22:6 PC ($T_c = -9.3$°C). In Fig. 1, DSC cooling scans are presented for pure DPPC (curve a), pure 18:0, 22:6 PC (curve k) and increasing mol% of 18:0, 22:6 PC in DPPC (curves b–j). Two transitions are seen. The higher melting component is primarily DPPC, while the lower melting component is primarily 18:0, 22:6 PC. Increasing mol% of 18:0, 22:6 PC decreases the enthalpy (ΔH), cooperativity, and phase transition temperature (T_c) of the higher melting DPPC-rich transition. By 50 mol% 18:0, 22:6 PC, the higher melting transition was greatly diminished and shifted by more than 10°C. Further increases of 18:0, 22:6 PC obliterated the DPPC-rich transition. The insert in Fig. 1 shows the effect of DPPC on DSC cooling

Table 1
Temperature (°C) of the main phase transition (T_c), ΔH (cal/mol), and cooperativity from the differential scanning calorimetry (DSC) cooling scans presented in Fig. 1 for MLV made from various mixtures of 18:0, 22:6 PC and DPPC

% 18:0, 22:6 PC in DPPC	High melting component			Low melting component		
	T_c (°C)	ΔH (cal/mol)	Cooperativity units	T_c (°C)	ΔH (cal/mol)	Cooperativity units
0	41.2	9039	1040.0	nd	nd	nd
10	39.9	8742	114.5	nd	nd	nd
20	38.2	6123	103.9	nd	nd	nd
30	36.8	4855	58.0	nd	nd	nd
40	33.9	6023	30.1	nd	nd	nd
50	28.9	880	24.4	−6.62	621	146.5
60	25.3	301	47.8	−7.16	602	70.6
70	21.4	1089	55.5	−7.60	1676	41.8
80	nd	nd	nd	−8.59	1994	66.4
90	nd	nd	nd	−9.01	3138	60.4
100	nd	nd	nd	−9.20	4405	173

nd, not detected.

scans of the lower melting, 18:0, 22:6 PC-rich transition. Increasing the mol% of DPPC decreases the enthalpy and cooperativity of this transition but has little effect on T_c. Table 1 summarizes ΔH, cooperativity and T_c for the various DPPC/18:0, 22:6 PC mixtures shown in Fig. 1. Although a low temperature phase transition was observed for mixtures containing more than 50 mol% 18:0, 22:6 PC in DPPC bilayers, no high temperature phase transitions ($\sim$30°C) were observed in these scans. A partial phase diagram was constructed from the DSC cooling scans and is reported in Fig. 2. Phase identification is similar to that reported by Bultmann et al. [32].

The DSC results presented in Figs. 1 and 2 demonstrate that DPPC/18:0, 22:6 PC mixtures exhibit monotectic behavior. At temperatures above 30–40°C, all lipids would be in the liquid crystalline state and below −10°C, all lipids would be in the gel state.

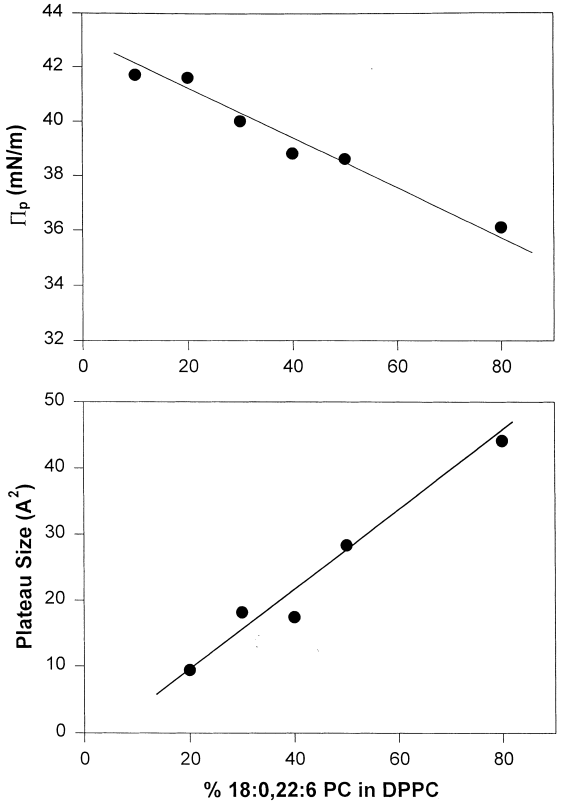

Fig. 4. Effect of increasing amounts of 18:0, 22:6 PC in DPPC monolayers on lateral pressure (Π_p, mN/m) where the plateau occurred (top panel) and the size of the plateau (expressed as changes in the mean molecular area, A^2) (bottom panel). Points are obtained from the pressure–area (Π–A) isotherms in Fig. 3.

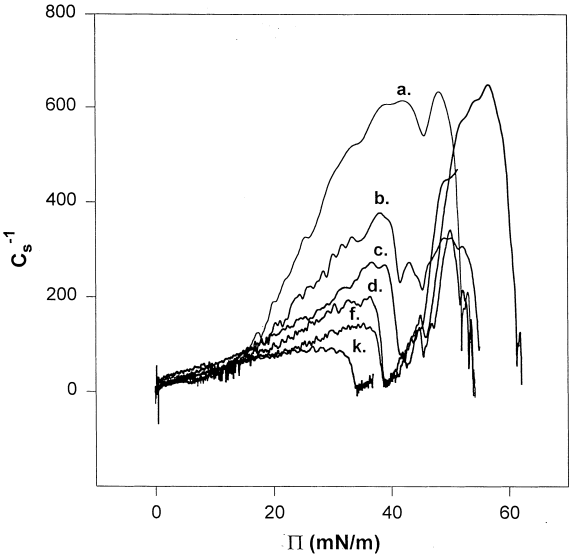

Fig. 5. Effect of increasing lateral pressure (mN/m) on surface elasticity moduli (C_s^{-1}) of various mixtures of DPPC/18:0, 22:6 PC. Curve a, 100 mol% DPPC; curve b, 90 mol% DPPC/10 mol% 18:0, 22:6 PC; curve c, 80 mol% DPPC/20 mol% 18:0, 22:6 PC; curve d, 70 mol% DPPC/30 mol% 18:0, 22:6 PC; curve f, 50 mol% DPPC/50 mol% 18:0, 22:6 PC; curve k, 100 mol% 18:0, 22:6 PC. Points are obtained from the pressure–area (Π–A) isotherms in Fig. 3.

Pressure–area (Π–A) isotherms of monolayers composed of the same lipid mixtures were then measured on a Langmuir trough. Fig. 3 presents Π–A isotherms of various mixtures of DPPC/18:0, 22:6 PC taken at 23°C. For mixed monolayers containing 20 mol% 18:0, 22:6 PC or more, there was a dramatic change in the Π–A curves with increasing lateral pressure. A 18:0, 22:6 PC-dependent plateau is quite obvious in these curves. The lateral pressure (Π_p, mN/m) where the plateau occurred (inflection point) and the size of the plateau (expressed as changes in the mean molecular area, A^2) were dependent upon the mol% of 18:0, 22:6 PC. Plateau size was determined by drawing a tangential line at the steep portion of the curve on either side of the plateau region of the Π–A isotherm. The distance between the two tangential lines was calculated for the plateau size where the Π–A isotherm curve intersected both tangential lines. Higher mol% of 18:0, 22:6 PC resulted in larger plateaus (Fig. 4, lower panel) and these plateaus formed at lower lateral pressures (Fig. 4, top panel). There was a dramatic increase in the Π–A slope after the plateau region

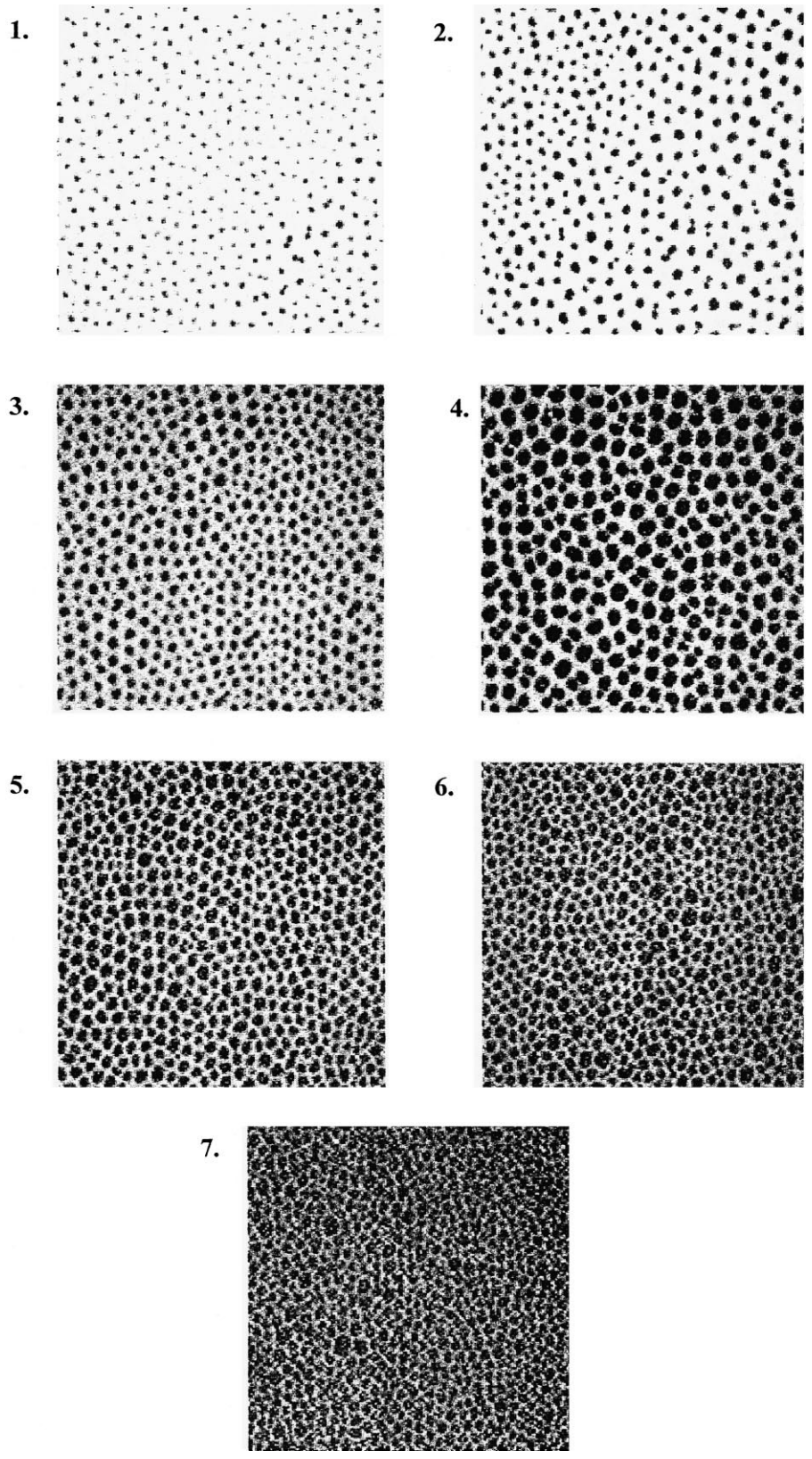
1.
2.
3.
4.
5.
6.
7.

Fig. 6. Epifluorescence microscopy images of monolayers composed of 29 mol% 18:0, 22:6 PC/70 mol% DPPC/1 mol% *N*-Rh-DOPE at various lateral pressures at 23°C. Images: 1, 5 mN/m; 2, 10 mN/m; 3, 15 mN/m; 4, 20 mN/m; 5, 25 mN/m; 6, 30 mN/m; and 7, 40 mN/m.
←

which continued until final monolayer collapse (curves c–f). The plateau represents the 'squeeze out' of the 18:0, 22:6 PC-rich monolayer component while the final monolayer collapse is the subsequent lateral pressure where the remaining DPPC-rich monolayer collapses. For mixtures containing pure DPPC and 90 mol% DPPC/10 mol% 18:0, 22:6 PC (Fig. 3, curves a and b), no plateau was observed. For the mixtures containing only 18:0, 22:6 PC and 80 mol% 18:0, 22:6 PC, there was an extended plateau region until the end of the run (curves i and k). Similar curves containing extended plateaus were also measured for the mixtures 40 mol% DPPC/60 mol% 18:0, 22:6 PC; 30 mol% DPPC/70 mol% 18:0, 22:6 PC; and 10 mol% DPPC/90 mol% 18:0, 22:6 PC (results not shown). Similar shaped 'plateaus' have been reported by Smaby et al. [31]. Surface elasticity modulus was calculated from each of these curves (Fig. 5). Depressions in the elasticity curves indicate dramatic changes in the slope of the *Π–A* isotherms and suggest a redistribution of lipids (changes in packing) within the monolayer [33,34].

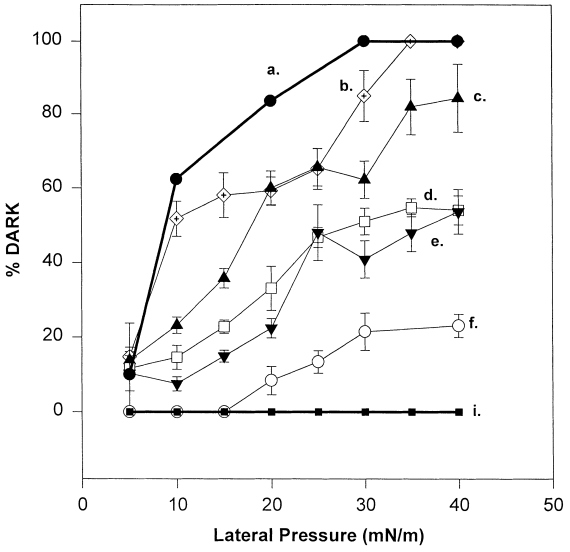

Fig. 7. Effect of increasing lateral pressure (mN/m) on % dark area for epifluorescent images of monolayers composed of: (a) 99 mol% DPPC/1 mol% *N*-Rh-DOPE; (b) 90 mol% DPPC/9 mol% 18:0, 22:6 PC/1 mol% *N*-Rh-DOPE; (c) 80 mol% DPPC/19 mol% 18:0, 22:6 PC/1 mol% *N*-Rh-DOPE; (d) 70 mol% DPPC/29 mol% 18:0, 22:6 PC/1 mol% *N*-Rh-DOPE; (e) 60 mol% DPPC/39 mol% 18:0, 22:6 PC/1 mol% *N*-Rh-DOPE; (f) 50 mol% DPPC/49 mol% 18:0, 22:6 PC/1 mol% *N*-Rh-DOPE; and (i) 99 mol% 18:0, 22:6 PC/1 mol% *N*-Rh-DOPE.

During monolayer compressions, lipid domains were imaged and quantified by fluorescence digital imaging microscopy using the rhodamine-labeled phospholipid, *N*-Rh-DOPE. In monolayers containing DPPC/18:0, 22:6 PC/*N*-Rh-DOPE, the fluorescent probe is expected to partition into the more fluid 18:0, 22:6 PC (liquid crystalline) phase [35,36]. Sample images in Fig. 6 are of a monolayer containing 70 mol% DPPC/29 mol% 18:0, 22:6 PC/1 mol% *N*-Rh-DOPE at lateral pressures between 5 and 40 mN/m. As the lateral pressure increased, the dark domains became larger and the total dark area relative to the total area of the image (% dark) increased (Fig. 7). The increase in % dark with increasing lateral pressure was observed only for mixtures containing 50 mol% or less of 18:0, 22:6 PC in DPPC (Fig. 7). At higher mol% of 18:0, 22:6 PC, no dark domains could be observed. At any lateral pressure, total dark area was also higher in mixtures of increasing mol% DPPC. Consequently, at any given lateral pressure, pure DPPC monolayers had the highest % dark area while pure 18:0, 22:6 PC monolayers had the lowest % dark. The imaging experiments clearly demonstrate lipid domains suggesting that lateral phase separation occurred in the DPPC/18:0, 22:6 PC mixed monolayers. The results also suggest that *N*-Rh-DOPE partitions into the 18:0, 22:6-PC-rich phase (the bright domains) and the dark domains exclude the probe and are DPPC-rich. In Fig. 8, the effect of increasing lateral pressure on average domain size was determined for several mixtures of DPPC/18:0, 22:6 PC. Results indicate that in monolayers containing 90 mol% DPPC/9 mol% 18:0, 22:6 PC/1 mol% *N*-Rh-DOPE and 80 mol% DPPC/19 mol% 18:0, 22:6 PC/1 mol% *N*-Rh-DOPE, there was a dramatic increase in the size of the domains at higher pressures (>20 mN/m) compared to mixtures containing 29–49 mol%

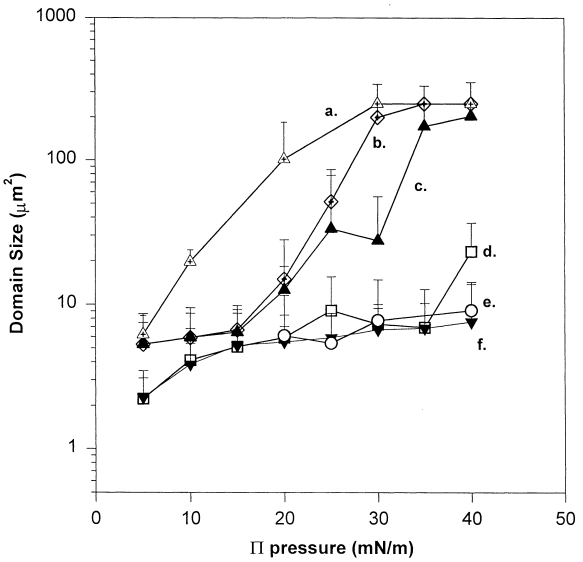

Fig. 8. Effect of increasing lateral pressure (mN/m) on average domain size ($i=15$) of monolayers composed of: (a) 99 mol% DPPC/1 mol% *N*-Rh-DOPE (b) 90 mol% DPPC/9 mol% 18:0, 22:6 PC/1 mol% *N*-Rh-DOPE; (c) 80 mol% DPPC/19 mol% 18:0, 22:6 PC/1 mol% *N*-Rh-DOPE; (d) 70 mol% DPPC/29 mol% 18:0, 22:6 PC/1 mol% *N*-Rh-DOPE; (e) 60 mol% DPPC/39 mol% 18:0, 22:6 PC/1 mol% *N*-Rh-DOPE; and (f) 50 mol% DPPC/49 mol% 18:0, 22:6 PC/1 mol% *N*-Rh-DOPE.

18:0, 22:6 PC. For 9 and 19 mol% 18:0, 22:6 PC in DPPC, at the highest lateral pressures, domains increased in size and therefore were in close proximity to one another. As domain size increased, our instrumentation had trouble distinguishing between many close small domains and one large fused domain. Regardless, this was not a problem for mixtures containing 29–49 mol% 18:0, 22:6 PC in DPPC as the size of the domains remained constant (approximately 10 μm^2).

4. Discussion

It is generally accepted that proteins and lipids in biological membranes are organized into discrete patches known as domains. Membrane domains are the consequence of poorly understood lipid–lipid and lipid–protein associations [1–3]. Although there has been much documentation on protein-driven domains, there is little known about lipid microdomains. This investigation focused on coexisting gel/liquid crystalline state lipid microdomains in lipid bilayers and monolayers composed in part of phosphatidylcholine (PC) containing the saturated fatty acid stearic acid in the *sn*-1 chain and docosahexaenoic acid (DHA) in the *sn*-2 chain. Differential scanning calorimetry studies (Figs. 1 and 2) indicated that DPPC/18:0, 22:6 PC bilayers phase separate. Next, pressure–area isotherms were measured on monolayers made from the same phospholipid mixtures used in the DSC experiments. Finally, monolayer lipid microdomains were visualized and quantified with fluorescence digital imaging microscopy. These experiments all indicate that the DPPC/18:0, 22:6 PC mixed membranes phase separate into DPPC-rich gel state and 18:0, 22:6 PC-rich liquid crystalline state domains. Demonstrating the involvement of a DHA-containing phospholipid in lipid domain formation in lipid bilayers and monolayers may serve as an initial step in providing evidence that DHA can induce phase separation in biological membranes as well.

Despite the recent advances in DRM studies, phase separation between gel and liquid-crystalline state lipids remains the best understood model for lipid microdomains in membranes. The techniques employed in the study presented have routinely been used to demonstrate lipid phase separations in model lipid bilayer membranes. DSC has often been the technique of choice in demonstrating phase separation in two component lipid bilayers [10,11,37]. Lipid monolayers have also been successfully employed in demonstrating gel/liquid crystalline phase separations. Changes in the slope of pressure–area isotherms suggest a lipid reorganization that is related to lateral phase separation [3]. Powerful visual evidence of gel/liquid crystalline state phase separation into domains in monolayers has also been provided through epifluorescence microscopy [38,39]. Several reports have indicated that monolayers containing gel phase, tightly packed lipids excluded large fluorescent chromophores, while phospholipid probes remain soluble in more disordered liquid crystalline regions of the film [35].

The majority of DSC studies [11,40–44] and many monolayer studies as well [30,35,45–47] have employed DPPC as the model phospholipid. Some of these experiments have been done to model the lung surfactant which is a DPPC-enriched monolayer [46,47] lining the interior of the lung and is involved

in reduction of surface tension during normal respiration. In surfactant studies, large changes in the slope of pressure–area isotherms were observed at higher pressures, indicating lipids being selectively excluded or 'squeezed out' from the monolayer. The concept of 'squeeze-out' has been described by Bangham [48] and others [30,35,45,49]. Bangham [48] demonstrated in two component monolayers that egg phosphatidylglycerol (egg PG) was 'squeezed out' leaving the monolayer enriched in DPPC. de Fontages et al. [49] and Boonman et al. [45] later demonstrated that 'squeeze out' of egg PG was enhanced by unsaturated acyl chains. Packing disruptions due to 'squeeze out' was also reported by Keough and coworkers [30,33] with monolayers composed of phospholipids and the lung surfactant proteins SP-B and SP-C. Taneva et al. [30] reported 'squeeze out' of SP-C and SP-B from DPPC/DPPG monolayers as followed by changes in surface elasticity modulus derived secondarily from pressure–area isotherms. It was suggested that the excluded phase contained SP-B since it was more disordered than DPPC/DPPG.

Since DHA is the longest and most unsaturated fatty acid commonly found in membranes [27], it is reasonable to assume that it might support unique functions not possible with other, shorter and less unsaturated fatty acids. A logical place to first search for a unique function for DHA would be in the membranes that normally are enriched in this fatty acid (rod outer segment, neuronal tissue and sperm) [28]. It has been postulated that DHA-containing phospholipids are a critical component of neuronal and optical function [28]. Niebylski et al. [50] have attributed DHA's role in neuronal tissue in part to its effect on acyl chain packing, reflecting the number and location of double bonds. NMR studies from Gawrisch and coworkers [26,51] have supported these conclusions. Using pyrene phospholipid fluorescence, Litman and Mitchell [24] demonstrated lateral phase separation in bilayers composed of DPPC/22:6, 22:6 PC. Salem and Niebylski [28] suggested that the membrane role of DHA incorporated into phospholipids in neuronal tissue was due to microdomain formation altering membrane physical properties.

The experiments presented here demonstrate lateral phase separation of co-existing gel-liquid crystalline lipids (DPPC/18:0, 22:6 PC) occurring in both lipid bilayers and monolayers. For lipid bilayers, lateral phase separation was detected by the presence of two transition peaks, a high temperature transition corresponding to high mol% of DPPC/low mol% 18:0, 22:6 PC and a low temperature transition corresponding to low mol% DPPC/high mol% 18:0, 22:6 PC (Fig. 1). The decrease in enthalpy as well as the shift in the transition temperatures for all lipid mixtures implies that the lipids are not completely immiscible [37]. Other authors have also shown that the saturated chain in mixed-chain DHA-containing phospholipids will preferentially interact with saturated chains on other phospholipids compared to DHA [25,26,52].

Pressure–area isotherms performed on the Langmuir–Blodgett trough indicate that mixtures of DPPC/18:0, 22:6 PC containing >20 mol% 18:0, 22:6 PC have breaks in the curve that can be attributed to exclusion or 'squeeze out' of lipid from the monolayer. The excluded lipid is primarily 18:0, 22:6 PC as suggested by the DHA-dependence on the lateral pressure where the Π–A break is first observed as well as on the size of the plateau (Fig. 4). The dips in surface elasticity curves (Fig. 5) are similar to those previously reported also demonstrating 'squeeze out' [30,31].

Images of domains formed as a function of lateral pressure in DPPC/18:0, 22:6 PC monolayers and visualized using a rhodamine-labeled phospholipid are presented in Fig. 6 and quantified in Fig. 7. It has often been reported from FRET studies that rhodamine-containing phospholipids will preferentially partition into the more disordered fluid (liquid crystalline) phase over the more ordered (gel) phase [36]. Moreover, DPPC-rich gel phases are known to exclude other fluorescent probes as well [35,39,40]. In a prior report using monolayers made from a lung surfactant extract (42% DPPC) and visualized by a *N*-Rh-DPPE probe, Discher et al. [36] described domains of liquid-ordered lipids surrounded by liquid-disordered domains. Bright fluorescent regions appeared suggesting separation of a distinct phase that contains the *N*-Rh-DPPE probe [36] which was consistent with our findings in this study. It is assumed then that the darker domains we observed in the DPPC/18:0, 22:6 PC mixtures are enriched in DPPC, while the bright domains containing the

rhodamine-moiety are enriched in 18:0, 22:6 PC. Both Nagg et al. [53] and Discher et al. [36] reported that during compression, the area of domains achieved a maximum value and then rapidly declined with further compression ($> \sim 35$ mN/m). In our mixtures, no reduction in the % dark area for mixtures between 0 and 50 mol% 18:0, 22:6 PC was noted from 0 to 40 mN/m (Fig. 7). Images were not taken at pressures above 40 mN/m, as the domains appeared to go out of the focal plane producing blurring which was difficult to capture with the CCD camera. 'Squeeze out' of 18:0, 22:6 PC from the monolayers occurred at >35 mN/m so it is possible that the difficulty in imaging we encountered at high pressures is the result of 'squeeze out' of both probe and the 18:0, 22:6 PC-rich phase.

For monolayers and bilayers containing >50 mol% 18:0, 22:6 PC in DPPC no dark, DPPC-rich domains could be visualized (Fig. 7) and the high temperature DSC transition (Fig. 1) was completely obliterated. All pressure–area isotherms containing >50 mol% 18:0, 22:6 PC were similar to the pressure–area isotherm of 20 mol% DPPC/80 mol% 18:0, 22:6 PC (shown in Fig. 3, curve i). These results suggest that at higher 18:0, 22:6 PC-mixtures, DPPC could be mixed homogeneously into the 18:0, 22:6 PC phase or if phase separation did occur, it was not detected by our methods (i.e. the domains were too small or maybe unstable). In mixtures containing 20–50 mol% 18:0, 22:6 PC at 23°C, there was a plateau region in the pressure–area isotherms followed by an increase in the slope suggesting that after 'squeeze out' of 18:0, 22:6 PC the remaining DPPC-enriched monolayer were further compressed (Fig. 3, curves c–f).

The results presented here demonstrate that phase separation of DPPC/18:0, 22:6 PC does occur for mixtures containing 50 mol% or less of 18:0, 22:6 PC in DPPC from ~ 0 to 20°C. In the future, we will apply these methods to more biologically relevant, liquid-ordered/liquid-disordered lipid mixtures to determine if one of the functions of DHA is to alter lipid microdomains in membrane.

Acknowledgements

This work was supported by Grant R01CA57212 from the National Institutes of Health and funds from the Phi Beta Psi Sorority.

References

[1] M. Edidin, Patches and fences: probing for plasma membrane domains, J. Cell Sci. 17 (Suppl.) (1993) 165–169.
[2] M. Glaser, Lipid domains in biological membranes, Curr. Opin. Struct. Biol. 3 (1993) 475–481.
[3] R.B. Gennis, Biomembranes, Springer-Verlag, New York, 1989, pp. 160–164.
[4] L.O. Bergelson, K. Gawrisch, J.A. Ferretti, R.E. Blumenthal, Special issue on domain organization in biological membranes, Mol. Membr. Biol. 12 (1995) 1–162.
[5] R. Welti, M. Glaser, Lipid domains in model and biological membranes, Chem. Phys. Lipids 73 (1994) 121–137.
[6] D.A. Brown, E. London, Structure and origin of ordered lipid domains in biological membranes, J. Membr. Biol. 164 (1998) 103–114.
[7] D.A. Brown, J.K. Rose, Sorting of GPI-anchored proteins to glycolipid-enriched membrane subdomains during transport to the apical cell surface, Cell 68 (1992) 533–544.
[8] J. Yu, D.A. Fischman, T.L. Steck, Selective solubilization of proteins and phospholipids from red blood cell membranes by nonionic detergents, J. Supramol. Struct. 3 (1973) 233–248.
[9] D.A. Brown, E. London, Function of lipid rafts in biological membranes, Annu. Rev. Dev. Biol. 14 (1998) 111–136.
[10] T. Heimberg, N.J. Ryba, U. Wurz, D. Marsh, Phase transition from a gel to a fluid phase of cubic symmetry in dimyristoylphosphatidylcholine/myristic acid (1, mol/mol) bilayers, Biochim. Biophys. Acta 1025 (2) (1990) 77–81.
[11] F. Lopez-Garcia, J. Villalain, J.C. Gomez-Fernandez, P.J. Quinn, The phase behavior of mixed aqueous dispersions of dipalmitoyl derivatives of phosphatidylcholine and diacylglycerol, Biophys. J. 66 (1994) 1991–2004.
[12] W. Stillwell, T. Dallman, A.C. Dumaual, F.T. Crump, L.J. Jenski, Cholesterol versus alpha-tocopherol effects on properties of bilayers made from heteroacid phosphatidylcholines, Biochemistry 35 (1996) 13353–13362.
[13] A.K. Hinderliter, J. Huang, G.W. Feigenson, Detection of phase separation in fluid phosphatidylserine/phosphatidylcholine mixtures, Biophys. J. 67 (1994) 1906–1911.
[14] D.E. Wolf, V.M. Maynard, C.A. McKinnon, D.L. Melchior, Lipid domains in the ram sperm plasma membrane demonstrated by differential scanning calorimetry, Proc. Natl. Acad. Sci. USA 87 (1990) 6893–6896.
[15] R.N. McElhaney, The structure and function of the *Acholeplasma laidlawii* plasma membrane, Biochim. Biophys. Acta 779 (1984) 1–42.
[16] J.E. Cronan, P.R. Vagelos, Metabolism and function of the membrane phospholipids of *Escherichia coli*, Biochim. Biophys. Acta 265 (1972) 25–60.
[17] R.N. Gilmore, N. Cohn, M. Glaser, Fluidity of LM cell

membranes with modified lipid compositions as determined with 1,6-diphenyl-1,3,5-hexatriene, Biochemistry 18 (1979) 1042–1049.
[18] T.M. Parasassi, M. Loiero, G. Raimondi, G. Rauagan, E. Gratton, Absence of lipid gel-phase domains in seven mammalian cell lines and in four primary cell types, Biochim. Biophys. Acta 1153 (1993) 143–154.
[19] W. Stillwell, S.R. Wassall, A.C. Dumaual, W. Ehringer, C.W. Browning, L.J. Jenski, Use of merocyanine (MC540) in quantifying lipid domains and packing in phospholipid vesicles and tumor cells, Biochim. Biophys. Acta 1146 (1993) 136–144.
[20] W. Stillwell, W. Ehringer, A.C. Dumaual, S.R. Wassall, Cholesterol condensation of α-linolenic and γ-linolenic acid-containing phosphatidylcholine monolayers and bilayers, Biochim. Biophys. Acta 1214 (1994) 131–136.
[21] A.A. Ribeiro, E.A. Dennis, PMR relaxation times of micelles of the nonionic surfactant Triton X-100 and mixed micelles with phospholipids, Chem. Phys. Lipids 14 (1975) 193–199.
[22] R.J. Schroeder, S.N. Ahmed, Y. Zhu, E. London, D.A. Brown, Cholesterol and sphingolipid enhance the Triton X-100 insolubility of glycosylphosphatidylinositol-anchored proteins by promoting the formation of detergent-insoluble ordered membrane domains, J. Biol. Chem. 273 (1998) 1150–1157.
[23] J.R. Silvius, D. del Giudice, M. Lafleur, Cholesterol at different bilayer concentrations can promote or antagonize lateral segregation of phospholipids of differing acyl chain length, Biochemistry 35 (1996) 15198–15208.
[24] B.J. Litman, D.C. Mitchell, A role for phospholipid polyunsaturation in modulating membrane protein function, Lipids 31 (1996) S193–197.
[25] L.L. Holte, F. Separovic, K. Gawrisch, Nuclear magnetic resonance investigation of hydrocarbon chain packing in bilayers of polyunsaturated phospholipids, Lipids 31 (1996) S199–S203.
[26] D. Huster, K. Arnold, K. Gawrisch, Influence of docosahexaenoic acid and cholesterol on lateral lipid organization in phospholipid mixtures, Biochemistry 37 (1998) 17299–17308.
[27] L.A. Whitting, C.C. Harvey, B. Century, M.K. Worwitt, Polyunsaturated lipids and α-tocopherol requirements, J. Lipid Res. 2 (1961) 412–418.
[28] N.J. Salem, C. Niebylski, The nervous system has an absolute molecular species requirement for proper function, Mol. Membr. Biol. 12 (1995) 131–134.
[29] C.D. Stubbs, The structure and function of docosahexaenoic acid in membranes, in: A. Sinclair, R. Gibson (Eds.), Essential Fatty Acids and Eicosanoids, American Oil Chemists' Society, Champaign, IL, 1992, pp. 116–121.
[30] S. Taneva, K.M.W. Keough, Pulmonary surfactant proteins SP-B and SP-C in spread monolayers at the air–water interface, Biophys. J. 66 (1994) 1137–1166.
[31] J.M. Smaby, M.M. Momsen, H.L. Brockman, R.E. Brown, Phosphatidylcholine acyl unsaturation modulates the decrease in interfacial elasticity induced by cholesterol, Biophys. J. 73 (1997) 1492–1505.
[32] T. Bultmann, W.L.C. Vaz, E.C.C. Melo, R.B. Sisk, T.E. Thompson, Fluid-phase connectivity and translational diffusion in a eutectic two-component, two-phase phosphatidylcholine bilayer, Biochemistry 30 (1991) 5573–5579.
[33] M.W. Hawco, P.J. Davis, K.M.W. Keough, Lipid fluidity in lung surfactant: monolayers of saturated and unsaturated lecithins, J. Appl. Physiol. Respirat. Environ. Exerc. Physiol. 51 (1981) 509–515.
[34] J. Egberts, H. Sloot, A. Mazure, Minimal surface tension, squeeze-out and transition temperatures of binary mixtures of dipalmitoylphosphatidlycholine and unsaturated phospholipids, Biochim. Biophys. Acta 1002 (1989) 109–113.
[35] C. Knobler, Seeing phenomena in flatland studies of monolayers of fluorescence microscopy, Science 249 (1990) 870–874.
[36] B.M. Discher, K.M. Maloney, W.R. Schief Jr., D.W. Grainger, S.B. Vogel, S.B. Hall, Lateral phase separation in interfacial films of pulmonary surfactant, Biophys. J. 71 (1996) 2583–2590.
[37] A.M. Jimenez-Monreal, J. Villalain, F.J. Aranda, J.C. Gomez-Fernandez, The phase behavior of aqueous dispersions of unsaturated mixtures of diacylglycerols and phospholipids, Biochim. Biophys. Acta 1373 (1998) 209–219.
[38] M. Losche, H. Mohwald, Impurity controlled phase transitions of phospholipid monolayers, Eur. Biophys. J. 11 (1984) 35–42.
[39] R. Peters, K. Beck, Translational diffusion in phospholipid monolayers measured by fluorescence microphotolysis, Proc. Natl. Acad. Sci. USA 80 (1983) 7183–7187.
[40] M.C. Phillips, B.D. Ladbrooke, D. Chapman, Molecular interactions in mixed lecithin systems, Biochim. Biophys. Acta 196 (1970).
[41] M. Schofield, L.J. Jenski, A.C. Dumaual, W. Stillwell, Cholesterol versus cholesterol sulfate: effects on properties of phospholipid bilayers containing docosahexaenoic acid, Chem. Phys. Lipids 95 (1998) 23–36.
[42] S. Mabrey, J.M. Sturtevant, Investigation of phase transitions of lipids, lipid mixtures by sensitivity differential scanning calorimetry, Proc. Natl. Acad. Sci. USA 73 (1976) 3862–3866.
[43] B.D. Ladbrooke, R.M. Williams, D. Chapman, Studies on lecithin–cholesterol–water interactions by differential scanning calorimetry and X-ray diffraction, Biochim. Biophys. Acta 150 (1968) 333–340.
[44] A. Blume, Phase transitions of polymerizable phospholipids, Chem. Phys. Lipids 57 (1991) 253–273.
[45] A. Boonman, F.H.J. Machiels, A.F.M. Snik, J. Egberts, Squeeze-out from mixed monolayers of dipalmitoylphosphatidylcholine and egg phosphatidylglycerol, J. Coll. Int. Sci. 120 (1987) 456–468.
[46] A.D. Bangham, Lung surfactant how it does and does not work, Lung 165 (1987) 17–25.
[47] J.N. Hildebran, J. Goerke, J.A. Clements, Pulmonary sur-

face film stability and composition, J. Appl. Physiol. Respirat. Environ. Exerc. Physiol. 47 (1979) 604–611.
[48] A.D. Bangham, C.J. Morley, M.C. Phillips, The physical properties of an effective lung surfactant, Biochim. Biophys. Acta 573 (1979) 552–556.
[49] A. de Fontages, F. Bonte, C. Taupin, R. Ober, Pressure–area curves of single and mixed monolayers of phospholipids and the possible relevance to properties of lung surfactant, J. Coll. Int. Sci. 101 (1984) 301–308.
[50] C.D. Niebylski, N.J. Salem, A calorimetric investigation of a series of mixed-chain polyunsaturated phosphatidylcholines: effect of sn-2 chain length and degree of unsaturation, Biophys. J. 67 (1994) 2387–2393.
[51] L. Holte, S. Peter, T. Sinnwell, K. Gawrisch, 2H nuclear magnetic resonance order parameter profiles suggest a change of molecular shape for phosphatidylcholines containing a polyunsaturated acyl chain, Biophys. J. 68 (1995) 2396–2403.
[52] B.W. Koenig, H.H. Strey, K. Gawrisch, Membrane lateral compressibility determined by NMR and x-ray diffraction: effect of acyl chain polyunsaturation, Biophys. J. 73 (1997) 1954–1966.
[53] K. Nagg, J. Perez-Gil, M.L. Ruano, L.A. Worthman, J. Stewart, C. Casals, K.M.W. Keough, Phase transitions in films of lung surfactant at the air–water interface, Biophys. J. 74 (1998) 2983–2995.